Polymer(Korea), Vol. 36, No. 4, pp. 542-548
http://dx.doi.org/10.7317/pk.2012.36.4.542

ISSN 0379-153X(Print)
ISSN 2234-8077(Online)

용매 어닐링에 의한 박막에서 Polystyrene-Poly(1,4-butadiene) 블록공중합체의 모폴로지 전이

이동은 · 김응건 · 이동현†
단국대학교 고분자시스템공학과
(2012년 5월 2일 접수, 2012년 5월 29일 수정, 2012년 5월 29일 채택)

Morphological Transitions of Symmetric Polystyrene-*block*-Poly(1,4-butadiene) Copolymers in Thin Films upon Solvent-Annealing

Dong-Eun Lee, Eung-Gun Kim, and Dong Hyun Lee†
Department of Polymer Science and Engineering, Dankook University, 126 Jookjeon-Dong, Suji-Gu, Yongin-Si, Gyeonggi-Do 448-701, Korea
(Received May 2, 2012; Revised May 29, 2012; Accepted May 29, 2012)

초록: 본 연구에서는 용매 증기 하에서 박막으로 제조된 polystyrene-poly(1,4-butadiene) 블록공중합체(PS-*b*-PBD)의 모폴로지 형성과 특성이 원자주사현미경(AFM)을 사용하여 연구되었다. 사이클로헥산으로만 용매 어닐링된 박막의 경우 폴리스티렌의 매트릭스 내부에 PBD가 미세상을 형성하는 perforated lamellae가 형성되었지만, *n*-헥산만으로 용매 어닐링 된 박막은 불규칙한 패턴만이 관측되었다. 그러나 사이클로헥산과 *n*-헥산의 혼합 용매를 사용하여 용매 어닐링할 경우 기질에 수직으로 배향된 라멜라가 관측되었다. 이러한 모폴로지 전이는 혼합 용매의 혼합비에 의해 조절되며 *n*-헥산의 양이 증가하면서 라멜라의 형성이 뚜렷이 관측되었다. 그러나 용매 어닐링에 사용된 혼합 용매 중 *n*-헥산의 주요 성분이 될 경우 *n*-헥산의 PBD로의 용매 친화력에 의해 모폴로지 형성이 오히려 지연되는 것을 확인하였다. 이러한 사이클로헥산과 *n*-헥산의 혼합비에 따른 모폴로지 전이는 블록공중합체에 대한 두 용매들의 친화력과 관련 있으며, 이를 이해하기 위해 이들의 용해도 상수 및 Flory 상호인력 인자들이 고려되었다. 또한 본 연구로부터 얻어진 두 가지 모폴로지를 이용하여 실리카 나노 패턴의 제조를 위한 템플레이트로 활용하였다.

Abstract: Morphological characteristics and formation of symmetric polystyrene-*block*-poly(1,4-butadiene) copolymer (PS-*b*-PBD) in thin films upon solvent-annealing were investigated by using atomic force microscopy (AFM). The thin films solvent-annealed in cyclohexane revealed the perforated lamellae of poly(1,4-butadiene) in the matrix of polystyrene while those solvent-annealed in *n*-hexane exhibited highly disordered patterns. Interestingly, when the thin films of PS-*b*-PBD were solvent-annealed with binary mixtures of cyclohexane and *n*-hexane, the morphological transition from the perforated lameallae to the perpendicularly-oriented lamellae of poly(1,4-butadiene) could be induced by changing the mixing ratio of both solvents. We also demonstrated that after microdomians of poly(1,4-butadiene) were successfully degraded by UV-O_3, linear poly(dimethyl siloxane) chains were back-filled into the etched regions of the thin film and then converted to silica nano-objects by oxygen plasma treatments.

Keywords: morphology, block copolymers, self-assembly, solvent-annealing, thin films.

Introduction

Block copolymers (BCPs) are capable of presenting a rich variety of well-ordered nanostructures including sphere, cylinder, lamella, etc. with periodic length in the range of 10-100 nm because of the immiscibility between chemically dissimilar polymers linked covalently at one end. Thus, BCPs have been considered as the potential candidates for nanotechnology and polymeric materials physics. In the bulk, BCP morphology can be determined by the total degree of polymerization (N), the volume fraction of one block (f_A), and the Flory-Huggins interaction parameter between the blocks (χ_{AB}).[1-3] On the other hand, in thin film, as additional parameters such as the film thickness and interfacial tension can play a significant role, it becomes more complicated to understand its morphology.[4-6] In

†To whom correspondence should be addressed.
E-mail: dlee@dankook.ac.kr

particular, such BCP nanostructures can provide many possible applications such as nanolithography,[6-8] ultra high-density data storage media,[9-11] nanostructured templates,[12,13] and photonic crystals[14] when they are prepared in thin films. In general, to take BCP morphology in thermodynamic equilibrium for the feasible applications mentioned above, the thin film is thermally annealed above the glass transition temperature (T_g) of both blocks, so that its ordering quality is improved and defect levels become reduced. However, the window of annealing temperatures for BCPs is normally limited because of their possible thermal degradation. Recently, some remarkable methods to achieve well-defined BCP ordering in large areas have been introduced, including interfacial interaction control,[5,15] electric field,[16,17] solvent vapor treatment,[18-23] chemically patterned substrate,[24] graphoepitaxy,[25] and epitaxial growth.[26]

The solvent-annealing, among several approaches introduced above, has advantages for practical reasons. Namely, this approach imparts a relatively simple and fast process to prepare highly ordered BCP nanostructures in large area as compared to others. In addition, this process does not need any preliminary treatment of BCPs and substrates. To induce their microphase separation, one only needs to control the evaporation of solvents from the film surface and the swelling degree of BCP microdomains. However, the interplay of solvents with blocks during solvent-annealing may affect extensively the existing thermodynamic parameters and make the system more complicated to understand. Hence, it is necessary to investigate the kinetics and mechanism of the solvent-annealing process for interesting BCPs.

Many research groups have reported the long-range ordering of a number of BCPs in the thin film after solvent-annealing treatment. The kinetics of polystyrene-*block*-polybutadiene-*block*-polystyrene (SBS) copolymers in thin solvent-cast films with different evaporation rates was investigated by Kim and Libera.[18] According to their results, the evaporation rate of solvents played an important role in determining the morphologies of SBS. The ordering behavior of different types of BCPs upon solvent-annealing was also studied. Krausch and coworkers conducted intensive studies on the morphological evolution of a polystyrene-*block*-poly(2-vinylpyridine-*block*-poly(*tert*-butyl methacrylate) copolymer induced by solvent-annealing.[19] They proved that the ordered nanostructures of BCPs developed from the film surface to the substrate due to the evaporation of solvent vapor. Recently, Russell and coworkers have reported the ordering and the orientation of cylindrical microdomains of a wide range of amphiphilic BCPs via solvent-annealing.[23,27,28]

In this study, we present the morphological transition of a symmetric polystyrene-*block*-poly(1,4-butadiene) copolymer (PS-*b*-PBD) in the thin film by solvent annealing with binary mixtures of cyclohexane (CHX) and *n*-hexane (HX). With varying composition of the solvent mixtures, transformation from the perforated lamellae to the perpendicularly-oriented lamellae was observed by atomic force microscopy (AFM). It was found that this transformation of PS-*b*-PBD microdomians was sensitively affected by the affinity of solvents for different blocks. Studies were performed as a function of the mixing ratio of both solvents and annealing time. In addition, we demonstrated that these well-defined nanostructures of PS-*b*-PBD thin films can be utilized as templates to produce nano-objects.

Experimental

Materials. The symmetric polystyrene-*block*-poly(1,4-butadiene) copolymer (PS-*b*-PBD, $M_{n,PS}$ = 19900 g/mol, $M_{n,PBD}$ = 22000 g/mol) was purchased from Polymer Source. And its polydispersity index (PDI) was 1.03. Poly(dimethyl siloxane) (PDMS, 10000 cSt.) was also purchased from Dow Corning. All polymers for this study were used without further purification. Cyclohexane (CHX) and *n*-hexane (HX) were purchased from Sigma-Aldrich and used as received without further purification. Si wafers (p-type, Si<100>) with a native silicon oxide layer were purchased from LG Siltron Inc. The pieces were 1.5 cm long and 1.5 cm wide.

Sample Preparation. Premeasured PS-*b*-PBD was dissolved in toluene at room temperature. The BCP solution was mechanically stirred for 24 hrs. Thin films of PS-*b*-PBD were spin-coated on Si substrates. Si substrates were cut into pieces with dimensions of 1 cm × 1 cm. To clean the surface of Si substrates before their use, they were first sonicated in acetone for 30 min and then exposed to UV-O_3 for 10 min. The BCP film thickness was controlled by changing concentration (0.7~1.5 wt%) of polymer solution and spin-coating rate and measured by ellipsometry. The BCP thin films were placed in a small closed vessel at ambient condition. To induce ordering of PS-*b*-PBD, 0.2 mL of either neat solvent (CHX or HX) or mixed solvent of CHX and HX was introduced into the chamber by a syringe. Finally, the BCP thin films were picked out from the chamber at a certain time of solvent-annealing and dried at room temperature.

Atomic Force Microscopy (AFM) Measurement. Surface topologies of PS-*b*-PBD thin films were assessed by atomic

force microscopy (Digital Instruments, Nanoscope III) in both the height and phase contrast operated in tapping mode. The *n*-doped Si tips (1-10 Ohm · cm) of Vecco were used to scan the surface of thin films in an area of 3 μm × 3 μm at a typical scan rate of 6 μm per second. The images obtained from all specimens were constructed using 512 scan lines.

UV-Ozone Treatment. The UV-Ozone generator was used to induce degradation of PBD blocks in thin film of PS-*b*-PBD. 6 mercury lamps (20 W × 6) were horizontally positioned on the top of the chamber in this generator. The distance from the surface of specimens to the lamps was approximately 10 cm. After certain doses of UV-O_3, the surface of thin films was washed with HX several times to extract degraded PBD chains and dried at ambient condition.

Fabrication of Silica Nanostructures. To fabricate silica nanodots and nanolines, linear poly(dimethyl siloxane) was dissolved in HX. A thin layer of PDMS was deposited by the spin-coating process on the thin film surface of PS-*b*-PBD that was treated by UV-O_3. As this specimen was thermally annealed at 70 °C for 30 min, PDMS was backfilled into the empty space generated by extracting PBD domains. To fabricate silica nanodots and nanolines, PDMS filled in pores was converted to silica by additional doses of oxygen plasma for 1 hr.

Results and Discussion

Figure 1 shows AFM images of the as-spun PS-*b*-PBD film. A thin film with 27.4 nm in thickness with a flat surface was achieved after spin-coating 1.0 wt% BCP/toluene solution on the Si substrate. However, as shown in Figure 1, highly disordered nanoscale structures were observed over the whole surface area. These disordered structures resulted from the incompatibility of two blocks during the spin-coating process, but have not fully developed because fast evaporation of solvents suppressed kinetically a microphase separation of block copolymers. Therefore, when the as-spun thin film of block copolymers is placed under certain circumstances to provide enough mobility to BCP chains such as the existence of solvent vapor, these chains can attain enough mobility and are able to continuously advance microphase separation of block copolymers. It is noted that some research groups reported that inversion of the contrast between PS and PBD, where the PS phase and PBD phase became dark and bright, respectively, could occur when the microscope was fulfilled at moderate tapping.[29,30] However, because our AFM experiments were operated at hard tapping, the glassy PS phase and rubbery PBD phase in phase mode of our AFM images appear as bright and dark regions, respectively.

As exhibited in Figure 2(a), in spite of their irregular ordering, discrete microdomains of PS-*b*-PBD were observed when the as-spun thin film was exposed to CHX vapor, which is a θ–solvent for PS blocks and a good solvent for PBD blocks, for 10 min. With further solvent-annealing (60 min), it was found that microdomains of PS-*b*-PBD were self-organized and then the perforated lamellae at a high degree of ordering were generated as shown in Figure 2(b). Even though CHX

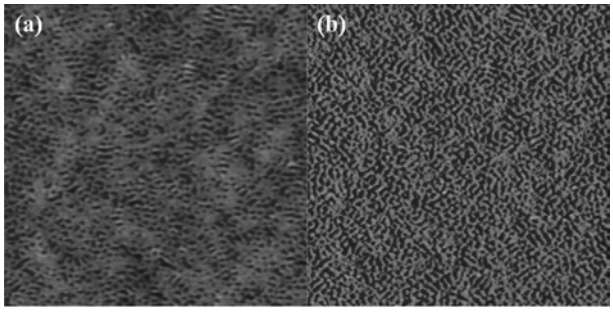

Figure 1. AFM images ((a) height mode; (b) phase mode, 1.5 μm × 1.5 μm) of the as-spun film of PS-*b*-PBD.

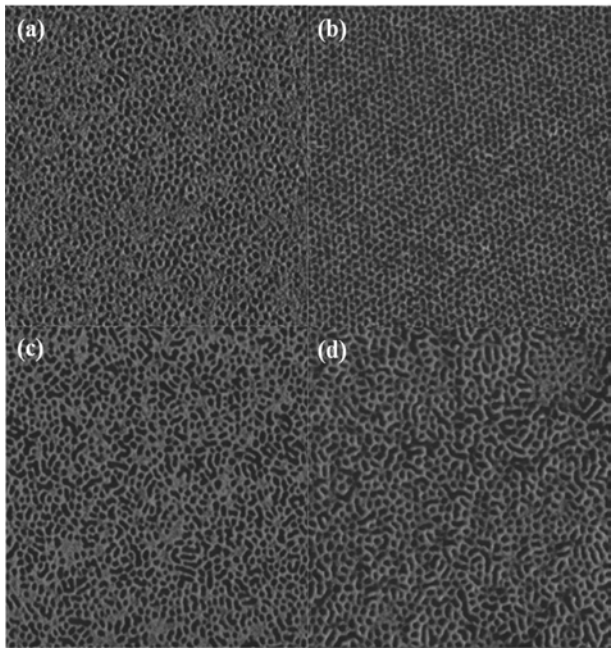

Figure 2. AFM images (phase mode, 1.5 μm × 1.5 μm) of PS-*b*-PBD thin films solvent-annealed in (a) cyclohexane for 10 min; (b) cyclohexane for 60 min; (c) *n*-hexane for 10 min; (d) *n*-hexane for 60 min, respectively.

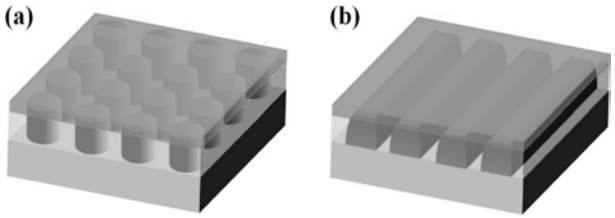

Scheme 1. A schematic illustration of the morphology of the thin films of polystyrene-*block*-poly(1,4-butadiene) copolymer solvent-annealed in vapor of a binary mixture of cyclohexane and *n*-hexane. (a) perforated lamellae; (b) perpendicularly-oriented lamellae, respectively. Dark and bright colors indicate PBD blocks and PS blocks, respectively.

has a higher affinity for the PBD block, according to our AFM results, PBD blocks formed the microdomains which are minor in the PS matrix. According to image analysis of AFM, the diameter of PBD domains was about 28 nm. The distance between the nearest microdomains of PBD was also around 38 nm. This phenomena may be related to the individual surface free energy of PS and PBD blocks. PBD chains tend to position at the surface of the film due to its lower surface free energy (32.5 mN/m) than that (36 mN/m) of PS chains.[31-34] Therefore, the BCP film is basically composed of two layers with the homogeneous PBD as the top layer and the PS and PBD blocks as the inhomogenous bottom layer (Scheme 1). To advance microphase separation between PS and PBD, PBD blocks may need to form microdomains in the PS matrix, which is the majority in the inhomogeneous bottom layer.

On the other hand, when the BCP thin film was exposed to HX which is selective solvent for PBD blocks for 10 min, irregularly ordered microdomains of PS-*b*-PBD were also generated (Figure 2(c)). After a solvent-annealing time of 60 min, PBD chains were dragged to the surface of the thin film by the vapor of HX while ill-defined structures still remained under the surface (Figure 2(d)).

He and coworkers conducted extensively the phase behavior of SBS and SB copolymer in thin films. They showed that slightly different affinities of solvents for blocks could dramatically affect their morphologies.[21,22,30] Moreover, the affinity of solvents for polymers is changeable in a given system. Therefore, it is essential to consider the relative affinity of solvents for BCPs systematically.

The relative affinity of solvents for each block can be adequately elucidated by the polymer-solvent interaction parameter ($\chi_{P\text{-}S}$) between the polymer (P) and the solvent (S) as shown in eq. (1).

$$\chi_{P-S} = V_S(\delta_S - \delta_P)^2/RT + 0.34 \quad (1)$$

where, V_s is the molar volume of the solvent, R is the gas constant, T is the temperature, and δ_S and δ_P are the solubility parameters of the solvent and the polymer, respectively. The solubility parameter of PS and PBD are 9.1 and 8.3 $cal^{1/2}/cm^{3/2}$, respectively. The calculated polymer-solvent interaction parameters ($\chi_{P\text{-}S}$) between individual blocks of PS-*b*-PBD and solvents are listed in Table 1.

For complete miscibility between polymer and solvent, the value of $\chi_{P\text{-}S}$ should be below 0.5 according to the Flory-Huggins criterion.[21-23,30] Thus, from the calculation of interaction parameters, it is seen that CHX used in this study is a θ-solvent for PS blocks and a good solvent for PBD blocks while HX is a selective solvent for only PBD blocks. Hence, CHX can provide a higher degree of swelling for PBD blocks than for PS blocks.

In addition, HX can swell only PBD blocks but does not affect PS blocks. To control the mobility of BCP chains as well as BCP ordering during the solvent-annealing process, it is a routine method to utilize mixtures of different solvents.[12,30] The morphological transition from the perforated lamellae to perpendicularly-oriented lamellae has been observed with increasing contents of HX in the binary mixture.

Figure 3 shows AFM images in phase mode of PS-*b*-PBD thin films that were solvent-annealed in binary mixtures of CHX and HX in different mixing ratios. When thin films were solvent-annealed in the vapor of a binary mixture of which majority is CHX, well-defined dot patterns of PS-*b*-PBD were still obtained (Figure 3(a)). However, with an increase of the HX concentration, it was found that discrete dots and continuous lines coexisted as shown in Figure 3(b). Interestingly, when the thin film of PS-*b*-PBD was exposed to the vapor of a binary mixture containing equivalent amounts of both solvents, highly ordered continuous-line patterns were achieved (Figure 3(c)). In contrast, irregularly ordered line and dot patterns were generated from the thin film that was solvent-

Table 1. Polymer-Solvent Interaction Parameters ($\chi_{P\text{-}S}$) between Blocks (P) of PS-*b*-PBD and Solvents (S)

	Cyclohexane	*n*-Hexane
Polystyrene	0.4981	1.0728
Poly(1,4-butadiene)	0.3426	0.5662

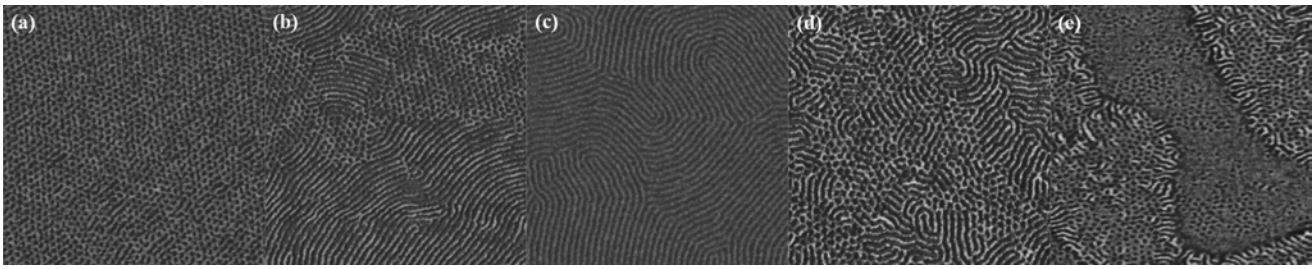

Figure 3 AFM images (phase mode, 1.5 μm × 1.5 μm) of PS-*b*-PBD thin films solvent-annealed in the binary mixtures of cyclohexane and *n*-hexane with various mixing ratios: (a) 90/10; (b) 70/30; (c) 50/50; (d) 30/70; (e) 10/90, respectively.

annealed in the vapor of a binary mixture with HX as the majority, as seen in Figure 3(d) and 3(e).

In order to trace morphological evolution of PS-*b*-PBD upon solvent-annealing, the AFM images of PS-*b*-PBD thin films were taken as a function of time during solvent-annealing in a binary mixture of CHX:HX = 50:50 (Figure 4). At the initial stage of the solvent-annealing process, highly disordered dot patterns of PBD blocks were formed in the matrix of PS blocks as shown in Figure 4(a). With further annealing (30 min), dot patterns congregated to form line patterns (Figure 4(b)). Then line patterns were observed eventually on the entire surface area after a solvent-annealing time of 1 hr (Figure 3(c)). The periodic distance of line patterns was about 35.3 nm. Therefore, we show that the combination of these two different solvents not only induce the link of PBD microdomains by swelling PBD blocks but also help maintain the perpendicular orientation of lamellae to the substrate. Significant changes of morphological characteristics were not observed even though they can also be affected by its thickness. Figure 5 displays AFM images of PS-*b*-PBD thin films of differing thickness that were solvent-annealed in a binary mixture (CHX:HX = 50:50) for 60 min. From the thin film with two different thicknesses of 14.4 nm (Figure 5(a)) and 54 nm (Figure 5(b)), well-defined lamellae oriented vertical to the substrate were also obtained.

Block copolymers have been regarded as possible templates to fabricate nanoscale features. Especially, block copolymers containing PBD blocks have been used as the mask for lithographic techniques because PBD blocks supply sufficient etching contrast for reactive ions like oxygen plasma or irradiation of UV-O_3. So, to confirm morphological characteristics of PS-*b*-PBD thin film in this study, PBD blocks were selectively etched after the thin films were exposed to UV-O_3. This etching treatment would reveal the exact position of PBD microdomains. As mentioned above, a homogeneous PBD layer

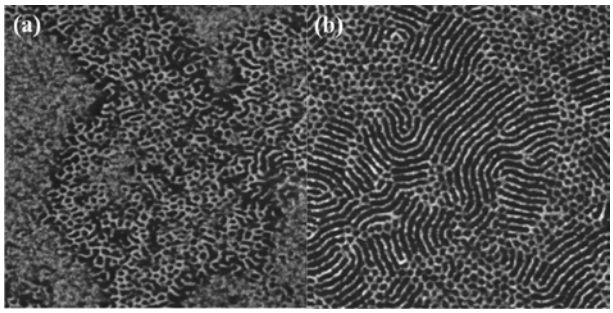

Figure 4. AFM images (phase mode, 1.5 μm × 1.5 μm) of PS-*b*-PBD thin films solvent-annealed in the vapor of the binary mixture of cyclohexane and *n*-hexane (50/50) with various annealing times: (a) 10 min; (b) 30 min, respectively.

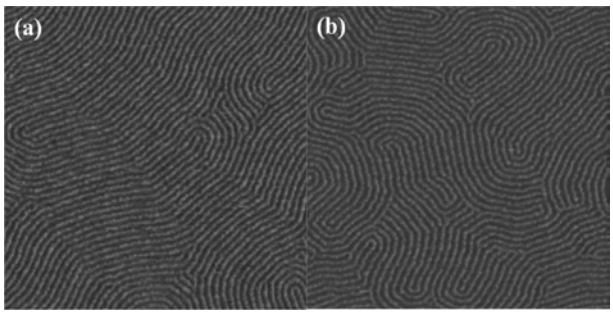

Figure 5. AFM images (phase mode, 1.5 μm × 1.5 μm) of PS-*b*-PBD thin films solvent-annealed in the binary mixtures of cyclohexane and *n*-hexane (50/50) with different thicknesses: (a) 12 nm; (b) 54 nm.

exists on the surface of thin films. As exhibited in Figure 6(a), this rubbery layer makes it difficult to see BCP morphology under the surface of the thin films. However, after exposure to UV-O_3 for 4 min, morphologies of PS-*b*-PBD thin films were successfully uncovered as shown in Figure 6(b) and 6(c). These highly ordered porous dot and line patterns corresponded to those in the AFM images given in Figure 2(b) and 3(c).

In nanolithography, BCPs containing inorganic components

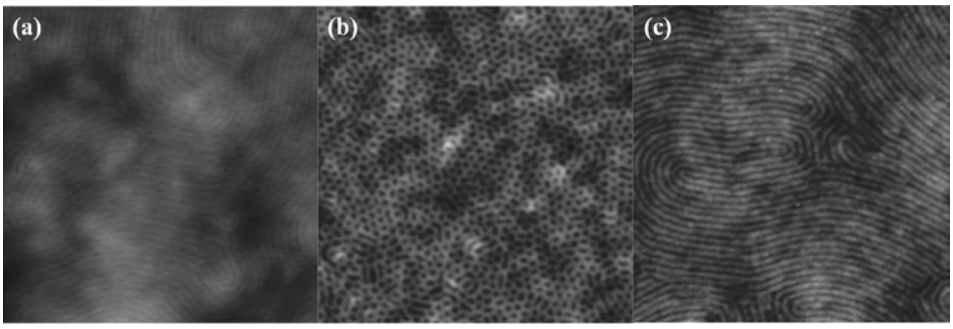

Figure 6. AFM images (height mode, 1.5 μm × 1.5 μm) of PS-*b*-PBD thin films (a) solvent-annealed in the binary mixtures of cyclohexane and *n*-hexane (50/50) for 1 hr, and its thin films exposed to UV-Ozone for (b) 30 sec; (c) 3 min.

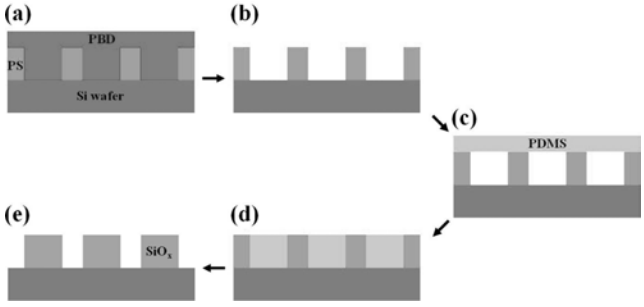

Scheme 2. A schematic illustration for fabrication of silica nano-objects. (a) solvent-annealed PS-*b*-PBD thin film; (b) UV-O_3 treated thin films; (c) spin-coated PDMS on porous thin film; (d) PDMS filled into pores; (e) silica nano-objects induced by oxygen plasma treatment.

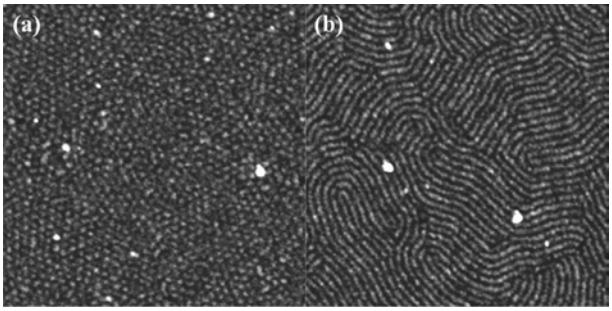

Figure 7. AFM images (height mode, 1.5 μm × 1.5 μm) of (a) silica nano-dots; (b) silica nano-lines.

are often used to fabricate inorganic nano-patterns via their self-assembly.[35] These types of BCPs can provide good ordering quality of their microdomains for even small-molecular-weight species due to their high values of χ between two blocks whereas the solvent-annealing for their microphase separation is very sensitive to the annealing condition involving types of solvent, substrates and humidity etc. and even requires pre-treated substrates. Hence, the use of BCPs exhibiting a higher etching contrast for one block is often preferred. PS-*b*-PBD can become one of the promising candidates for this practical reason. As mentioned above, PBD blocks can be degradable easily during the traditional etching process. Thus, these porous thin films could be used as a desirable template to fabricate silica nanodots and nanolines. As linear PDMS was spin-coated on these porous thin films obtained from UV-O_3 etching and thermally annealed at 70 °C for 30 min, PDMS chains were backfilled into the pores due to the capillary force. When these backfilled films were exposed to oxygen plasma, the organic part of the remaining BCP film was degraded while PDMS was converted to silica. Consequently, silica nano-dots and nanolines were fabricated (Scheme 2).

Figure 7(a) and 7(b) show AFM images (height mode) of highly ordered silica nanodots and nanolines, respectively. Thus, it is confirmed that arrays of silica nano-objects were successfully produced without changing the dimensions of the original BCP templates.

Conclusions

Morphological transitions of symmetric polystyrene-*block*-poly(1,4-butadiene) copolymers from the perforated lamellae to perpendicularly-oriented lamellae were investigated upon solvent-annealing. The perforated lamellar structures of the thin film were developed in the vapor of pure cyclohexane which is the θ–solvent for PS block and a good solvent for PBD block while ill-defined structures of PS-*b*-PBD were obtained in the vapor of *n*-hexane, a selective solvent for PBD block. In contrast, as the film was solvent-annealed in the binary mixture of cyclohexane and *n*-hexane, perpendicularly-oriented lamellae were produced. All transitions occurred without significant changes in size and separation distance of PBD microdomains. In addition, the PS-*b*-PBD thin film with

highly ordered nanoscale structures were successfully utilized as a template to fabricate silica nano-objects by using conversion from PDMS to silica as induced by oxygen plasma treatment.

Acknowledgement: The present research was conducted by the research fund of Dankook University in 2011.

References

1. I. W. Hamley, T*he Physics of Block Copolymers*, Oxford Science Publications, New York, 1998.
2. L. Leibler, *Macromolecules*, **13**, 1602 (1980).
3. F. S. Bates and G. H. Fredrickson, *Annu. Rev. Phys. Chem.*, **41**, 525 (1990).
4. A. Knoll, A. Horvat, K. S. Lyakhova, G. Krausch, J. A. Sevink, A. V. Zvelindovsky, and R. Magerle, *Phys. Rev. Lett.*, **89**, 0355011 (2002).
5. P. Mansky, Y. Liu, E. Huang, T. P. Russell, and C. J. Hawker, *Science*, **275**, 1458 (1997).
6. C. J. Hawker and T. P. Russell, *MRS Bull.*, **30**, 952 (2005).
7. C. Tang, E. M. Lennon, G. H. Fredrickson, E. J. Kramer, and K. J. Hawker, *Science*, **322**, 429 (2008).
8. S. Park, D. H. Lee, J. Xu, B. Kim, S. W. Hong, U. Jeong, T. Xu, and T. P. Russell, *Science*, **323**, 1030 (2009).
9. W. Lee, H. Han, A. Lotnyk, M. A. Schubert, S. Senz, M. Alexe, D. Hesse, S. Baik, and U. Gösele, *Nat. Nanotechnol.*, **3**, 402 (2008).
10. J. Y. Cheng, C. A. Ross, C. Z.-H. Chan, E. L. Thomas, R. G. H. Lammertink, and G. J. Vancso, *Adv. Mater.*, **13**, 1174 (2001).
11. T. Thurn-Albrecht, J. Schotter, G. A. Kästle, N. Emley, T. Shibauchi, L. Krusin-Elbaum, K. Guarini, C. T. Black, M. T. Tuominen, and T. P. Russell, *Science*, **290**, 2126 (2000).
12. D. H. Lee, S. Park, W. Gu, and T. P. Russell, *ACS Nano*, **5**, 1207 (2011).
13. H. Cho, S. Choi, J. Y. Kim, and S. Park, *Nanoscale*, **3**, 5007 (2011).
14. A. C. Edrington, A. M. Urbas, P. DeRege, C. X. Chen, T. M. Swager, N. Hadjichristidis, M. Xenidou, L. J. Fetters, J. D. Joannopoulos, Y. Fink, and E. L. Thomas, *Adv. Mater.*, **13**, 421 (2001).
15. I. In, Y. H. La, S. M. Park, P. F. Nealey, and P. Gopalan, *Langmuir*, **22**, 7855 (2006).
16. T. L. Morkved, M. Lu, A. M. Urbas, E. E. Ehrichs, H. M. Jaeger, P. Mansky, and T. P. Russell, *Science*, **16**, 931 (1996).
17. T. Thurn-Albrecht, J. DeRouchey, T. P. Russell, and H. M. Jaeger, *Macromolecules*, **33**, 3250 (2000).
18. G. Kim and M. Libera, *Macromolecules*, **31**, 2569 (1998).
19. K. Fukunanga, H. Elbs, R. Magerle, and G. Krausch, *Macromolecules*, **33**, 947 (2000).
20. S. Niu and R. F. Saraf, *Macromolecules*, **36**, 2428 (2003).
21. Q. Zhang, O. K. C. Tsui, B. Du, F. Zhang, T. Tang, and T. He, *Macromolecules*, **33**, 9561 (2000).
22. H. Huang, F. Zhang, Z. Hu, B. Du, T. He, F. K. Lee, Y. Wang, and O. K. C. Tsui, *Macromolecules*, **36**, 4084 (2003).
23. S. Park, J. Wang, B. Kim, W. Chen, and T. P. Russell, *Macromolecules*, **40,** 9059 (2007).
24. S. O. Kim, H. H. Solak, M. P. Stoykovich, M. J. Ferrier, J. J. de Pablo, and P. F. Nealey, *Nature*, **424**, 411 (2003).
25. R. A. Segalman, H. Yokoyama, and E. J. Kramer, *Adv. Mater.*, **13**, 1152 (2001).
26. C. De Rosa, C. Park, E. L. Thomas, and B. Lotz, *Nature*, **405**, 433 (2000).
27. S. H. Kim, M. J. Misner, and T. P. Russell, *Adv. Mater.*, **16**, 2119 (2004).
28. K. A. Cavicchi and T. P. Russell, *Macromolecules*, **40**, 1181 (2007).
29. A. Knoll, R. Magerle, and G. Krausch, *Macromolecules*, **34**, 4159 (2001).
30. H. Huang, Z. Hu, Y. Chen, F. Zhang, Y. Gong, and T. He, *Macromolecules*, **37**, 6523 (2004).
31. L. H. Lee, *J. Polym. Sci.*, **5**, 1103 (1967).
32. E. A. Grulke, "VII Solution Properties", in *Polymer Handbook*, J. Brandrup and E. H. Immergut, Editors, John Wiley & Son, New York, p 176 (1989).
33. M. G. Buonomenna, G. Golemme, C. M. Tone, M. P. De Santo, F. Ciuchi, and E. Perrotta, *Adv. Funct. Mater.*, **22**, 1759 (2012).
34. A. Turturrot, E. Gattiglia, P. Vacca, and G. T. Viola, *Polymer*, **36**, 3987 (1995).
35. Y. S. Jung, J. B. Chang, E. Verploegen, K. K. Berggren, and C. A. Ross, *Nano Lett.*, **10**, 1000 (2010).